Accuracy of DTFT-based Sine-wave Amplitude Estimators

Daniel Belega[1], **Dario Petri**[2], **and Dominique Dallet**[3]
[1]Department of Measurements and Optical Electronics, University Politehnica Timişoara, Bv. V. Pârvan, Nr. 2, 300223, Timişoara, Romania
[2]Department of Industrial Engineering, University of Trento, Trento 38123, Italy
[3]IMS Laboratory, Bordeaux IPB, University of Bordeaux, CNRS UMR5218, 352, 351 Cours de la Libération, Bâtiment A31, 33405, Talence Cedex, France

E-mail: daniel.belega@upt.ro, dario.petri@unitn.it, dominique.dallet@ims-bordeaux.fr

Abstract. In this paper the accuracies of the sine-wave amplitude estimators provided by three state-of-the-art Discrete Time Fourier Transform (DTFT)-based algorithms are compared each other when a small number of cycles is acquired and the input signal is affected by wide-band noise. These algorithms allow to reduce the detrimental contribution of the spectral image component by processing specific Discrete Fourier Transform (DFT) samples using frequency-domain interpolation and the least-squares method. Two algorithms are based on two- and three-point Interpolated DFT (IpDFT) procedure, respectively. The third algorithm applies the least-squares approach to three DTFT samples in order to reduce also the contribution of wide-band noise. The robustness of the related amplitude estimators to sine-wave frequency uncertainty and wide-band noise is also investigated.

1. Introduction

Real-time and accurate knowledge of sine-wave parameters is required in many engineering applications, such as in control and monitoring systems. Frequency-domain procedures based on the Discrete Time Fourier Transform (DTFT) are often employed to this aim due to their very good performance. One widely used procedure is the so-called Interpolated Discrete Fourier Transform (IpDFT) algorithm [1-6]. That algorithm estimates the sine-wave inter-bin frequency location by interpolating the two highest DFT samples of the input signal weighted by a suitable window function in order to reduce spectral leakage. The sine-wave amplitude and phase are then estimated by using the highest DFT sample and the estimated inter-bin frequency location. Simple analytical expressions for the sine-wave parameter estimators have been derived when the Maximum Sidelobe Decay (MSD) cosine windows [7] are employed [1, 3, 4]. Moreover, these windows exhibit an optimum sidelobe decay rate, thus ensuring very good spectral leakage reduction [2, 3]. Unfortunately, when the number of acquired sine-wave cycles is small, as occurs when a fast algorithm response is required, the IpDFT estimators can be strongly affected by the contribution of the spectral image component [3, 4]. To overcome this problem different IpDFT frequency and amplitude estimators based on the MSD windows have been proposed [8-11]. A two point IpDFT procedure, called in the following 2pIpDFT-IC algorithm, provides accurate amplitude estimates by compensating the contribution of the image component on the considered DFT samples [9]. Another procedure, the 3pIpDFT-IR, considers finite

differences of the highest three DFT samples with the aim of reducing the effect of the spectral image component on the estimated sine-wave amplitude [10]. Another recently proposed method to reduce that detrimental contribution is the so called enhanced Frequency-domain Linear Least-Squares (e-FLLS) amplitude estimator [11]. That algorithm allows also to minimize the effect of wide-band noise on the obtained estimates, since it is based on rectangular windowing and the least-squares method. A comparison of the effectiveness of the amplitude estimators listed above in reducing the contribution of the spectral image component has not yet performed in the scientific literature. This is the aim of this paper, which analyses the achievable accuracy in the case when a fast response time is required, so that only a small number of sine-wave cycles can be observed. Also, the robustness of the obtained amplitude estimators to sine-wave frequency uncertainty and wide-band noise is investigated in this following.

2. The considered DTFT-based amplitude estimators

Let's consider the discrete-time noisy sine-wave expressed by:

$$x(m) = A\sin(2\pi f m + \phi) + e(m) = A\sin\left(2\pi\frac{\nu}{M}m + \phi\right) + e(m), \quad m = 0,1,2,\dots,M-1 \qquad (1)$$

where A, f, and ϕ are its amplitude, normalized frequency, and initial phase, $e(\cdot)$ is a discrete-time white Gaussian noise with zero mean and variance σ^2, and M is the acquisition length. The normalized frequency, defined as the ratio between the frequency f_{in} of the original continuous-time sine-wave and the sampling rate f_s, is equal to: $f = \nu/M = (l + \kappa)/M$, where ν is the number of acquired sine-wave cycles, l is its integer part, and κ ($-0.5 \le \kappa < 0.5$) is the inter-bin frequency location. In practice κ is often not null, that is non-coherent sampling occurs [12].

To reduce the spectral leakage due to the finite duration of the observation interval and non-coherent sampling, signal (1) is weighted by an H-term MSD window [7]. The DTFT of the achieved windowed signal $x_w(m) = x(m)\cdot w(m)$ is given by:

$$X_w(\lambda) = \sum_{m=0}^{M-1} x_w(m)e^{-j2\pi\frac{\lambda}{M}m} = \frac{A}{2j}\left[W(\lambda-\nu)e^{j\phi} - W(\lambda+\nu)e^{-j\phi}\right] + E_w(\lambda), \quad \lambda \in [0, M) \qquad (2)$$

where $W(\cdot)$ and $E_w(\cdot)$ are the DTFTs of the window $w(\cdot)$ and the weighted wide-band noise $e_w(m) = x(m)\cdot w(m)$ respectively.

The amplitude estimators provided by the 2pIpDFT-IC, the 3pIpDFT-IR, and the e-FLLS algorithms are given by (3), (4), and (5), respectively [9-11]:

$$\hat{A}_{2p,c} = \frac{H+(-1)^s\hat{\kappa}}{(2H-1)(l+\hat{\kappa})}\cdot\frac{(2l+\hat{\kappa}+(-1)^s(H-1))|X_w(l)|+(2l+\hat{\kappa}+(-1)^{s+1}H)|X_w(l+(-1)^{s+1})|}{|W(\hat{\kappa})|}, \qquad (3)$$

where $s = 0$ if $|X_w(l-1)| > |X_w(l+1)|$ and $s = 1$ if $|X_w(l-1)| < |X_w(l+1)|$;

$$\hat{A}_{3p,r} = \frac{H^2-\hat{\kappa}^2}{H(2H-1)}\frac{|X_w(l-1)|+2|X_w(l)|+|X_w(l+1)|}{|W(\hat{\kappa})|}, \qquad (4)$$

$$\hat{A}_{3p,e} = 2\left|X_w(l+\hat{\kappa}) - \frac{W_R(2l+2\hat{\kappa})[W_R^*(2l+2\hat{\kappa}-1)X_w(l+\hat{\kappa}-1)+W_R^*(2l+2\hat{\kappa}+1)X_w(l+\hat{\kappa}+1)]}{|W_R(2l+2\hat{\kappa}-1)|^2+|W_R(2l+2\hat{\kappa}+1)|^2}\right|, \qquad (5)$$

where $W_R(\lambda) = \sum_{m=0}^{M-1} e^{-j2\pi\frac{\lambda}{M}m}$ is the DTFT of the rectangular window and $(\cdot)^*$ denotes the complex conjugate operator. In (3) – (5), $\hat{\kappa}$ represents the available estimate of the inter-bin frequency location.

3. Amplitude estimation accuracy comparison

In this Section the accuracies of the amplitude estimators $\hat{A}_{2p,c}$, $\hat{A}_{3p,r}$, and $\hat{A}_{3p,e}$ are compared each other by means of computer simulations. Both pure and noisy sine-waves are considered and $1.5 < \nu < 6$ cycles are observed. In the IpDFT algorithms the Hann window is used. Sine-waves are characterized by amplitude $A = 1$ and initial phase ϕ that varies at random in the range $[0, 2\pi)$ rad. Monte Carlo simulations composed by 1000 runs of $M = 512$ samples each have been performed.

3.1. Pure sine-waves

Fig. 1 shows the magnitude of the amplitude errors returned by the considered estimators as a function of ν when the inter-bin frequency location κ is known (Fig. 1(a)), estimated by the three-point IpDFT algorithm [8] (Fig. 1(b)) or estimated by the classical IpDFT algorithm [2, 4] (Fig. 1(c)). Notice that the frequency estimation accuracy decreases when moving from Fig. 1(a) to Fig. 1(c).

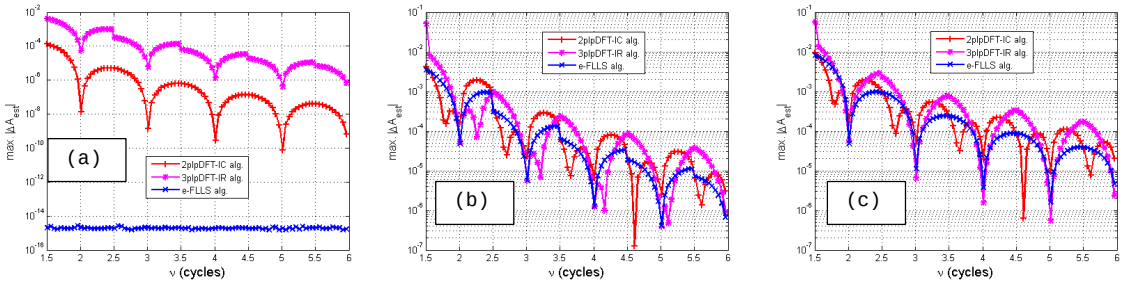

Figure 1. Pure sine-waves: Magnitude of the estimation errors returned by the estimators $\hat{A}_{2p,c}$, $\hat{A}_{3p,r}$, and $\hat{A}_{3p,e}$ versus the number of observed cycles ν when the inter-bin frequency location κ is known (a), estimated by the three-parameter IpDFT algorithm [8] (b), or estimated by the IpDFT algorithm [2, 4] (c).

When the sine-wave frequency is known, Figure 1(a) shows that the $\hat{A}_{3p,e}$ estimator outperforms the others. Also, the accuracy of that estimator almost doesn't depend on the number of observed cycles and it is very small. Conversely, Figures 1(b) and (c) show that the estimator $\hat{A}_{3p,e}$ exhibits a higher sensitivity to sine-wave frequency uncertainty. Indeed, there exist values of ν where the estimators $\hat{A}_{2p,c}$ and $\hat{A}_{3p,r}$ provide more accurate results.

3.2. Noisy sine-waves

Fig. 2 shows the Mean Square Error (MSE) of the considered amplitude estimators as a function of ν when noisy sine-waves characterized by *SNR* = 40 dB are analysed; the same inter-bin frequency location estimators adopted in Figure 1 (b) and (c) are used in Figures 2(b) and (c). The Cramér-Rao Lower Bound (CRLB) for unbiased amplitude estimators, that is $(\sigma_A^2)_{CR} \cong 2\sigma^2/M$ [3], is also shown in Figure 2 for comparison.

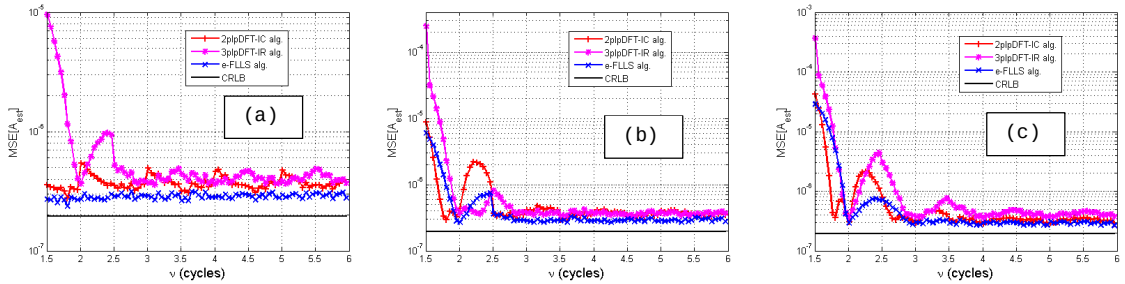

Figure 2. Noisy sine-waves: MSEs returned by the amplitude estimators $\hat{A}_{2p,c}$, $\hat{A}_{3p,r}$, and $\hat{A}_{3p,e}$ versus the number of observed cycles ν when the inter-bin frequency location κ is known (a), estimated by the three-parameter IpDFT algorithm [8] (b), or estimated by the IpDFT algorithm [2, 4] (c).

As it can be observed, when the sine-wave frequency is known, the $\hat{A}_{3p,e}$ estimator outperforms the others and its MSE is almost independent of the number of observed cycles. When the accuracy of the estimated sine-wave frequency decreases, the behaviour of the curves in Figures 2(b) and (c) reproduce

those shown in Figure 1(b) when $\nu < 2.5$ cycles or Figure 1(c) when $\nu < 3$ cycles, respectively. Indeed, in the analysed conditions, the contribution of the spectral image component on the considered spectral samples dominates the effect of noise. As a consequence, there exist values of ν where the estimators $\hat{A}_{2p,c}$ and $\hat{A}_{3p,r}$ outperform the estimator $\hat{A}_{3p,e}$. For greater values of ν, the contribution of wide-band noise dominates and the estimator $\hat{A}_{3p,e}$ ensures the best accuracy. In particular, the related MSE is close to $1.5\,(\sigma_A^2)_{CR}$ [10]. It is worth noticing that simulations always returned behaviours similar to those reported in Figure 2 for any *SNR* value higher than 10 dB, even though the value of ν up to which the contribution of the spectral image component overcomes the effect of noise increases as *SNR* increases.

4. Conclusions

Simulation results showed that the e-FLLS sine-wave amplitude estimator [11], which is based on the least-squares approach and rectangular windowing, exhibits a better accuracy than both the two- and three-point IpDFT algorithms 2pIpDFT-IC [9] and 3pIpDFT-IR [10] when the contribution of wide-band noise prevails on the effect of the spectral image component. Conversely, when this later disturbance prevails and the sine-wave frequency is known with high accuracy, the 2pIpDFT-IC and the 3pIpDFT-IR algorithms can outperform the e-FLLS estimator.

References

[1] Rife D C and Vincent GA 1970 *Use of the discrete Fourier transform in the measurement of frequencies and levels of tones, Bell Syst. Tech. J.* **49** 197-228.

[2] Grandke T 1983 *Interpolation algorithms for discrete Fourier transforms of weighted signals, IEEE Trans. Instrum. Meas.* **32** 350-5.

[3] Offelli C and Petri D 1992 *The influence of windowing on the accuracy of multifrequency signal parameter estimation, IEEE Trans. Instrum. Meas.* **41** 256-61.

[4] Belega D and Dallet D 2009 *Multifrequency signal analysis by interpolated DFT method with maximum sidelobe decay windows, Measurement* **42** 420-6.

[5] Quinn B G 1997 *Estimation of frequency, amplitude, and phase from the DFT of a time series, IEEE Trans. Signal Process.* **45** 814-817.

[6] Duda K and Barczentewicz S 2014 *Interpolated DFT for sin$^{\alpha}$ windows, IEEE Trans. Instrum. Meas.* **63** 754-60.

[7] Nuttall A H 1981 *Some windows with very good sidelobe behavior, IEEE Trans. Acoust. Speech Signal Process.* **ASSP-29** 84–91.

[8] Agrež D 2007 *Dynamic of frequency estimation in the frequency domain, IEEE Trans. Instrum. Meas.* **56** 2111-8.

[9] Belega D, Dallet D and Petri D 2014 *Sine-wave amplitude estimation by a two-point interpolated DFT method robust to spectral interference from the image component IMEKO Conference Proceedings* 709-13.

[10] Agrež D 2002 *Weighted multipoint interpolated DFT to improve amplitude estimation of multifrequency signal, IEEE Trans. Instrum. Meas.* **51** 287-92.

[11] Belega D, Petri D and Dallet D 2018 *Amplitude and phase estimation of real-valued sine-wave via frequency-domain linear least-squares algorithms, IEEE Trans. Instrum. Meas.* **67** 1065-77.

[12] Ferrero R and Ottoboni R 1992 *High-accuracy Fourier analysis based on synchronous sampling techniques, IEEE IEEE Trans. Instrum. Meas.* **41** 780-5.